

DETERMINATION OF AERODYNAMIC DAMPING OF AXIAL-COMPRESSOR-BLADES USING A BIDIRECTIONAL FLUID-STRUCTURE-SIMULATION

A. KÜHHORN, S. SCHRAPE, J. NIPKAU

Brandenburg University of Technology, Chair of Structural Mechanics and Vehicle Vibrational Technology
Siemens-Halske-Ring 14, D-03046 Cottbus
Germany

ABSTRACT

The present work deals with the analysis of the aeroelastic behaviour of a 2D subsonic compressor cascade which has been derived from a real high pressure compressor (meanline approach). The main focus is on the determination of the aerodynamic damping as well as the frequency shifts of damped blade vibrations with regard to varying interblade phase angles. The analysis comprises different methods of determining the aerodynamic damping by means of fluid-structure coupled simulations. Therefore a partitioned fluid-structure coupling approach is used to couple two separate codes, one CFD-code and one FEM-code, via a third-party coupling interface. Furthermore one method is presented for the determination of the aerodynamic damping by making only use of the CFD-code. The calculations comprise the solution of the unsteady Reynolds-averaged Navier Stokes (RANS) equations in combination with the Spalart-Allmaras turbulence model on so called hybrid meshes. The structural model consists of up to five single-degree-of-freedom (SDOF) models representing the blade vibrations in an idealised flap mode. The code-coupling is done in an explicit manner using a sequential coupling algorithm. The results are shown to be highly dependent on the proper choice of the type of boundary conditions while different physical approaches for the determination of the aerodynamic damping lead to similar results.

INTRODUCTION

In order to achieve an effective reduction of fuel consumption and lower manufacturing costs in aviation, integrated lightweight design solutions have been developed for aero engines during the last years. In order to satisfy those requirements with innovative high-pressure compressors the application of blade integrated disks (Blisk) plays an essential role. Blisks are characterised by lower mechanical damping values compared to the separated blade-disk design. Though the various mechanisms of aerodynamic excitation remain unaffected by the blade-disk design. Therefore the lower mechanical damping of the integrated design negatively affects the high cycle fatigue (HCF). Additionally geometrical and material imperfections (mistuning) lead to localised vibrational modes which are characterised by concentrations of vibrational energy in a few blades. These phenomena could even worsen the problem of higher amplification factors and critical stress and strain levels. Further influences occur from fluid-structure interaction. By excluding flutter phenomena from the

current investigations, an attenuation of strong localisations may be expected. To ensure a safe and predictable operation, an improved comprehension of the complex fluid-structure interactions and the resulting blade vibration behaviour becomes necessary.

The Chair of Structural Mechanics and Vehicle Vibrational Technology has experienced 6 years of work concerning experimental and numerical investigations related to blisk vibrational technology [2], [3], [4]. In order to study the effect of the airflow on the structural forced vibration response a current research project deals with an especially developed Equivalent-Blisk-Model (EBM) composed of lumped masses, spring and damper elements, which has been proved by experimental studies and numerical results from a FEM analysis [2]. For the intention of integrating aerodynamic elements in the structural EBM, the knowledge of additional airflow effects, such as aerodynamic damping, frequency shift caused by additional moving air mass as well as stiffening effects between adjacent blades, especially by oscillating out of phase, are essential. Therefore the influence of the blade surrounding airflow is simulated by an explicit, partitioned fluid-structure coupling approach using the coupling tool MpCCI (Mesh based parallel Code Coupling Interface) [20]. FIG. 1 shows an idealised scheme of such an EBM. The basic simulation model used within this work consists of a simplified 2D subsonic compressor cascade vibrating in the first flap mode. In terms of the EBM an identification of the aerodynamic elements finally requires the results of fully coupled FSI analysis.

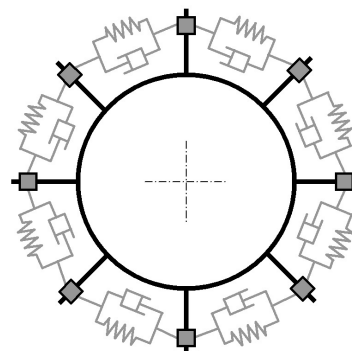


FIG. 1. Aerodynamic elements in an idealised scheme of an Equivalent Blisk Model

1. PHYSICAL AND NUMERICAL MODEL

1.1. Compressor Cascade Configuration

Due to intensive numerical and experimental investigations concerning the structural dynamics of a real blisk rotor including mistuning effects during the recent years, the intention of studying the aerodynamic influence on blades, which vibrate as a result of engine order excitation, is well founded. Therefore all simulations presented subsequently make use of a simplified model representing the same blisk geometry of one of the last stages of a real high pressure test compressor (FIG. 2).

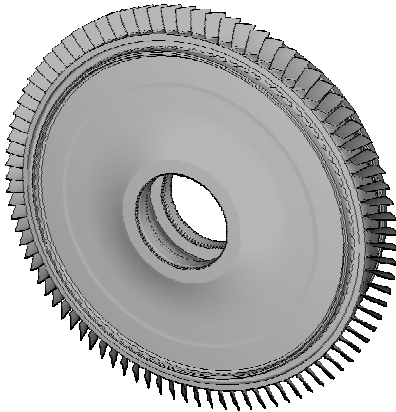


FIG. 2. Blisk rotor

The basic model represents a meanline approach of those rotor blades at 50% span. FIG. 3 pictures the original 3D blade, which corresponds to the geometry the meanline blade geometry is derived from. Thereby it is important to use the deflected blade shape with respect to the applied operating condition taking into account the influences of rotor speed and steady pressure distribution on the blade's surface. In the aerodynamic design process boundary conditions only make sense in combination with blade definitions representing the running blade shape of the hot blade. That is why all ambient conditions of the blade flow essentially affect the aerodynamic results. The operating conditions used herein are desired to result maximum component loads at forced response. This requirement usually leads to the maximum-take-off (MTO) boundary conditions.

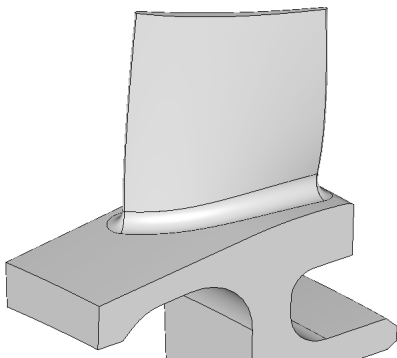


FIG. 3. 3D blade

In a physical consideration of forward (FTW) and backward travelling waves (BTW) which are described in chapter 1.3, the interblade phase angle (IBPA) dependent aerodynamic damping has to be calculated for the chosen boundary conditions.

1.2. Coupling Concept

In order to cover the effects of the airflow on the structural position of the blade on the one hand and the interaction of the change in blade position on the airflow on the other hand, a coupling of the usually separately treated disciplines of structural dynamics and fluid dynamics becomes necessary, this is referred to as Fluid-Structure-Interaction (FSI). A first classification of the coupling algorithms results in the distinction of unidirectional and bi-directional procedures. These differ in a way that with the unidirectional procedure the change of the flow due to the small structural deformations is so small that it can be neglected. Assuming a negligible influence of the flow variables on the structural movement the unidirectional transfer of the structural deformations to the flow solver is possible as well. This approach is also used herein in order to compare it with the results of bi-directional coupled calculations and is shown in FIG. 4.

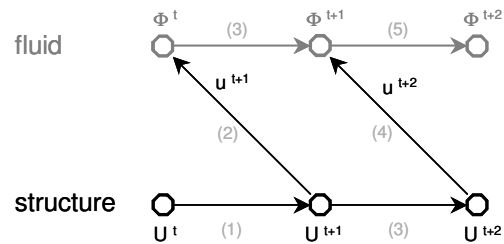


FIG. 4. Unidirectional coupling algorithm

Here Φ represents the flow solution and U the solution of the structural calculations. The discrete time steps are indicated by the superscript t , $t+1$, $t+2$ and so on. The chronology of operations is specified by the light grey numbers in parentheses. Only the FEM-code transfers the internal calculated structural deformations to the CFD-code. That way an unsteady boundary condition for the flow solver is realised. If the CFD-code contains an interface for the implementation of such boundary conditions, this procedure does not essentially require a third party coupling interface.

In contrast, the bi-directional procedure takes the change of the structural deformation, due to the now no more negligible flow, into account. The bilateral exchange of the coupling variables takes place in an explicit manner meaning one exchange in each time step. It is schematically shown in FIG. 5. The time delay of the explicit (weak) coupling algorithm is responsible for the fact that the coupling conditions (geometric compatibility of fluid and structure as well as compatibility of boundary conditions at the interface) are not fulfilled exactly. Therefore, relatively small time increments have to be chosen to achieve stability and equilibrium.

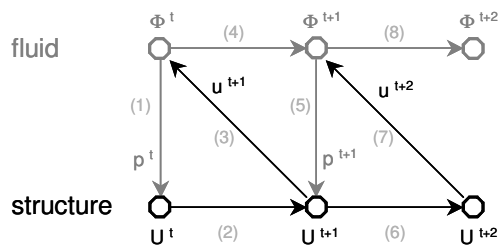


FIG. 5. Bi-directional coupling algorithm

The CFD-code transfers the computed pressure distribution p to the FEM-code, which calculates a structural displacement u applying this pressure load. With the structural displacement u the fluid mesh is updated and a new pressure distribution is computed in the following step.

Depending on the physical strength of Fluid-Structure-Interaction problems it should be distinguished between explicit (weakly coupled) and implicit (strongly coupled) algorithms. On the contrary to the explicit coupling the coupling conditions are completely fulfilled when using the implicit method. This is realised via an iterative connection of the sub-problems. Thus the stability and energy conservation of the partitioned coupling approach are improved. In a time step the iterations continue until a predefined convergence criterion is satisfied and a so-called dynamic equilibrium evolves. A more precise, but the same time more complex computation of strongly coupled phenomena succeeds by means of a monolithic coupling. Fluid and structural domain are identically discretised resulting in a description by the same equations which are solved simultaneously in one code.

In the present work an explicit, partitioned coupling approach via MpCCI (Mesh based parallel Code Coupling Interface, developed by the Fraunhofer Institute SCAI) is mainly used to exchange data between the FE-code ABAQUS for the structural part and the CFD-code FLUENT for the part of the fluid. With explicit methods quantities of flow and structure are exchanged in a staggered manner. That way the full range of code capabilities without specific model restrictions such as modal simplification can be used. By doing so the transfer as well as the interpolation of mesh based quantities is provided by the MpCCI coupling server. Due to the different spatial discretisation the interface regions are identified applying mapping schemes based on neighbourhood search algorithms. Displacements are interpolated from the structural mesh onto the fluid mesh in a non-conservative way making use of the local coordinates as well as finite element trial functions. The interpolation of fluid-forces onto the structural mesh bases on force weighting procedures related to the finite element trial functions. Thereby it works in a conservative manner. Further details about the interpolation-procedures employed in the MpCCI-Interface can be found in [18].

1.3. Structural Model

Within this work only tuned blade-assemblies are going to be considered which exhibit typical Cyclic Symmetry Modes (CSM). These so called double modes have identical eigenfrequencies and natural modeshapes. These natural modeshapes differ only in the angular

distribution of their Nodal Diameter (ND) lines. Such systems can have complex eigenvectors due to their cyclic system matrices. The resulting complex modes do not only possess individual amplitudes, but also individual phase angles. The displacement characteristic corresponds to that of a real mode for IBPA=0° and IBPA=180° (standing waves), while the complex modes describe travelling waves over the perimeter (0° > IBPA > 180°). Complex modes can be distinguished into forward (FTW) and backward travelling waves (BTW), where positive IBPA lead to forward travelling waves and negative IBPA to backward travelling waves looking into the positive direction of rotation. So the interblade phase angle dependent aerodynamic damping is going to be computed using a multipassage approach representing a 2D compressor cascade model. FIG. 6 exemplarily shows a model of three passages with an illustration of a backward travelling wave.

At first, for reasons of model simplifications, only blade vibrations in 1st flap mode are admitted (local 2 direction) in the current work. In the two dimensional approach this vibration mode leads to a pure bending vibration without any torsional component. From the mechanical point of view the blade is modelled as a "Single Degree of Freedom Oscillator". By adjusting mass and stiffness of the model the first flap related eigenfrequency of the simulated 3D blade is defined.

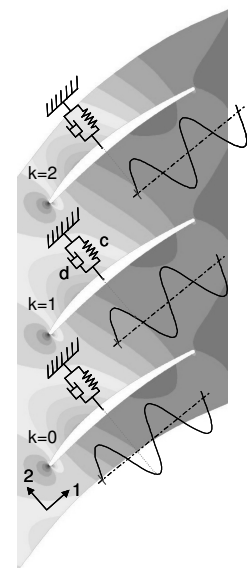


FIG. 6. Aeroelastic model 120°, BTW

Within the reduction of the real blade to the 2D blade only the half blade mass was used when considering the first flap mode. In order to be able to correctly calculate the fluid forces which react on the blade, the use of a blade height becomes necessary even in a 2D approach. The fluid forces directly depend on the coupled surface and thus on the blade height. As a first approximation half the value of the real blade height is used.

For the simulation in ABAQUS each blade movement can be defined separately. Defining a reference blade (k=0) the oscillations of all indicated blades of the undamped system can be specified by the following formula:

$$(1) \quad u_k(t) = \sin(\omega t + k \cdot \text{IBPA}); \quad \text{IBPA} = 360^\circ \frac{\text{ND}}{N}.$$

Here k denotes the blade index and N means the total number of blades of the real blisk and the computational model respectively.

In the range of small displacements the aerodynamic damping is regarded to be independent of the actual size of the displacement, hence a limitation of the

displacement amplitude for aeroelastic computations appears to be reasonable. From a structural mechanics point of view the worst case occurs when the amplitudes of the forced oscillations lead to a load within the range of the endurance limit of 100% (HCF-Endurance). That's why the maximum endurable amplitude of the 3D blade at 50% span was specifically calculated for the employed eigenfrequency. For smaller amplitudes it is assumed that the aerodynamic damping is independent of the displacement amplitude.

The spatial discretisation is done with linear plane stress elements, which are superposed by rigid elements to model the assumed rigid body blade model. The linear elements are only required by the interpolation algorithms of the coupling interface. The FE-code solves the ordinary differential equations of motion with mass and stiffness as defined beforehand without any structural damping. By doing so damping forces only come from the equations' right hand sides and thus from the computation of the CFD-code. Thereby a dynamic computation is done using an explicit central difference time integration scheme. Here a modified Leapfrog algorithm of second order accuracy is used. Node velocities are computed using half time steps while node displacements and accelerations are computed using full time steps.

Finally it needs to be noted that regarding fully coupled calculations the steady lift of the steady fluid computations has to be compensated in the structural part of the coupled calculations. The blade geometries used within the coupled calculations already correspond to the running blade shape at the beginning of the calculations. If the steady lift forces are not compensated an additional displacement would result in perturbations of the initial blade movement. The importance of this compensation originates from the blade movement being an essential part which is needed to excite the aerodynamic modes according to the interblade phase angles which are going to be investigated.

1.4. Flow Model

The flow model employed in this work bases on a two-dimensional, viscous, compressible (ideal gas) and time-dependently flow, which is going to be computed with the CFD-code FLUENT. The flow is described using the Reynolds averaged form of the continuity equation, momentum conservation equation and energy conservation equation in combination with the Spalart-Allmaras one-equation turbulence model.

By simulating the subsequent FSI problem, moving boundaries of the structure within the fluid domain have to be taken into consideration. Therefore the so called Arbitrary-Lagrangian-Eulerian formulation (ALE) is used, which gives a correct mathematical description of flow problems including moving grids. Equation (2) describes the integral form of the transport equation for a general scalar Φ on a moving arbitrary control volume V with the surface A :

$$(2) \quad \frac{d}{dt} \int_V \rho \Phi dV + \int_A \rho \Phi (\mathbf{u} - \mathbf{u}_g) \cdot \mathbf{dA} = \int_A \Gamma \nabla \cdot \Phi \mathbf{dA} + \int_V S_\Phi dV,$$

where ρ is the fluid density, \mathbf{u} is the absolute fluid velocity vector (Euler velocity), \mathbf{u}_g is the velocity vector of the

moving grid, Γ is the diffusion coefficient and S_Φ is the source term of Φ . The convective and diffusive terms are discretised using the Finite Volume Method. The particular problem definition doesn't include any sources. That's why the source term of equation (2) isn't taken into account.

The time integration is done using an unsteady implicit time stepping method (dual-time-formulation) of 1st order accuracy (Euler backward). For a physical time step the constitutional change can be solved in the pseudo time level by implicit or explicit integration. In case of non-reflecting boundary conditions, which are described below, the pseudo time is explicitly integrated with a 3-stage Runge Kutta method. Otherwise the integration is done in an implicit manner.

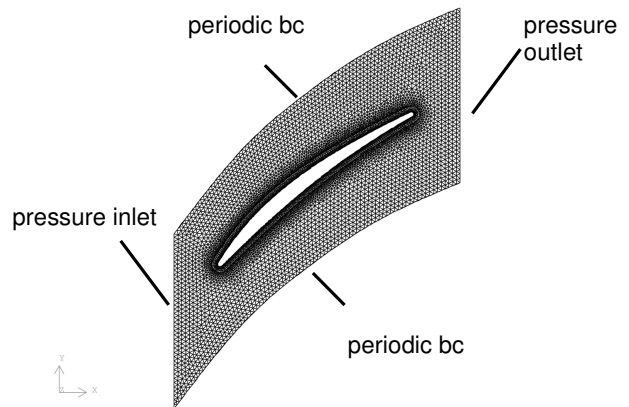


FIG. 7. Single passage

FIG. 7 displays a single passage of the rotor blade with the appropriate boundary conditions. At the pressure inlet the total pressure, the total temperature and the inlet flow angle are prescribed. At the pressure outlet the static pressure is held constant. The lateral borders of the flow domain are defined as translational, periodic boundaries with respect to the two-dimensional compressor cascade approach. The periodic boundaries enable us to compute different IBPA's by varying the number of blade passages, the IBPA=90° can be calculated by using 4 passages for example. The boundary condition variables depend on the chosen operating condition. In addition to the maximum-take-off conditions at the start of an airplane, computations of cruise conditions are regarded. The cruise conditions differ from the MTO conditions concerning the flight altitude and the speed in cruise flight. For unsteady computations there are also some non-reflecting boundary conditions implemented in FLUENT which will be used in addition to the standard boundary conditions. They can only be assigned to pressure outlets and work with characteristic wave relations derived from the Euler equations. Because this special treatment is formulated in an inviscid and one-dimensional way, all transversal and viscous wave components not looking into the orthogonal direction of the pressure outlet boundary will be neglected. This leads to simplified compatibility conditions which do not represent exact "physical" conditions [19].

The computational mesh is of hybrid type and consists of a structured boundary layer mesh (O-Mesh) in the vicinity of the blade's surface while the rest of the flow domain is meshed in an unstructured fashion, as shown in FIG. 7. The blade movement requires the deformation of the mesh which can be realised in FLUENT by remeshing and smoothing techniques [8] in combination with quality checks of characteristic mesh features like equiangle-skewness and the element size.

To complete the description of the flow model its worth mentioning that the steady state solution is used as initial value for the unsteady computations. Furthermore the steady solution is needed to identify the steady lift which has to be compensated.

2. DAMPING DETERMINATION

The different methods used herein differ from one another in the way the blade-movement is achieved, the way the damping value is calculated, the coupling algorithm which is applied and the participating codes respectively.

2.1. Coupling Algorithms

For problems involving large displacements and/or large fluid forces the influences can't be neglected anymore and proper results can only be obtained by taking the full complexity of Fluid-Structure-Interaction into account.

2.1.1. Bi-directional coupling

The bi-directional coupling requires the use of both simulation codes which take part in the partitioned coupling algorithm. As explained in the previous section the blade-displacement is supposed to be at the limit of the maximum endurable amplitude to reach one hundred percent endurance. Due to this relatively large displacement the interaction between blade-flow and blade-vibration is regarded not to be negligible.

The actual intention of determining the aerodynamic damping requires the movement of the blades in the flow, which can be achieved by two principal techniques, they are

- a) The blades are subjected to phase dependent, initial conditions (initial displacement, velocity or acceleration). Afterwards they are left alone performing free, damped vibrations.
- b) The blades are subjected to a phase and time dependent sinusoidal force-, velocity- or displacement signal which leads to a forced response blade-vibration. After the blades have reached their steady state vibration condition they are left alone performing free, damped vibrations.

Referring to a):

Depending on the interblade phase angle an initial displacement along with an initial velocity make up an entire initial state for each blade, from which each blade starts its individual free, damped vibration. Starting with the solution of the undamped (the mechanical damping is excluded in all analyses) single degree of freedom

equation of motion

$$(3) \quad m\ddot{u}_k + cu_k = 0,$$

where m and c are the mass of the k -th blade and the stiffness respectively. Since only tuned blade-assemblies are going to be analysed, mass and stiffness are the same for every blade. With the initial conditions $u_k(t=0) = u_{k,0}$ and $\dot{u}_k(t=0) = \dot{u}_{k,0}$ one obtains the solution for the displacement of the k -th blade as follows

$$(4) \quad u_k(t) = u_{k,0} \cos(\omega \cdot t) + \frac{\dot{u}_{k,0}}{\omega} \sin(\omega \cdot t).$$

Defining one reference blade with $k=0$ the displacement of the k -th blade depending on the initial conditions of the reference blade becomes

$$(5) \quad u_k(t) = u_{0,0} \cos(\omega \cdot t + k \cdot \text{IBPA}) + \frac{\dot{u}_{0,0}}{\omega} \sin(\omega \cdot t + k \cdot \text{IBPA})$$

For the initial state with $t=0$, equation (5) provides the initial displacement for the k -th blade with

$$(6) \quad u_k(t=0) = u_{0,0} \cos(k \cdot \text{IBPA}) + \frac{\dot{u}_{0,0}}{\omega} \sin(k \cdot \text{IBPA}).$$

Differentiating equation (5) one yields the time dependent velocity of the k -th blade connected to the initial conditions of the reference blade, namely

$$(7) \quad \frac{du_k}{dt}(t) = -u_{0,0} \cdot \omega \cdot \sin(\omega \cdot t + k \cdot \text{IBPA}) + \dot{u}_{0,0} \cos(\omega \cdot t + k \cdot \text{IBPA})$$

which leads to the initial velocity of the k -th blade in the form of

$$(8) \quad \dot{u}_k(t=0) = -u_{0,0} \cdot \omega \cdot \sin(k \cdot \text{IBPA}) + \dot{u}_{0,0} \cdot \omega \cdot \cos(k \cdot \text{IBPA}).$$

With equations (6) and (8) a set of initial conditions is available which allow a calculation of initially excited blade vibrations. With time advancing these vibrations will be damped due to the surrounding airflow, hence an evaluation of the logarithmic decrement of the decaying blade amplitudes can lead to the aerodynamic damping ratio of the k -th blade according to the following equation

$$(9) \quad \Lambda_k = \frac{1}{m} \ln \frac{u_k(t)}{u_k(t+m \cdot T)} = \frac{2\pi D_k}{\sqrt{1-D_k^2}},$$

where m means the number of cycles between the decay is to be considered. For $D < 0.3$ equation (9) can be linearised as follows

$$(10) \quad \frac{2\pi D_k}{\sqrt{1-D_k^2}} \approx 2\pi D_k \quad \text{and therefore} \quad D_k \approx \frac{\Lambda_k}{2\pi}.$$

The main disadvantages of this method are the complex setup and pre-processing steps to prepare the matching blade positions in ABAQUS and FLUENT, the choice of the proper force for lift-compensation and the resulting perturbations introduced into the flow which decay slowly depending on the strength of convection within the flow.

Referring to b):

The second method avoids the disadvantages of the preceding one, but it has its main drawback in the much greater calculation effort. Typically 5 to 10 times more time is needed compared to the first method.

The basic idea of this method is to force the blades with the undamped system's eigenfrequency into the desired phase-shifted vibrations until a steady state vibration (with respect to a constant amplitude) is reached. After having reached this steady state, the forcing is removed and the blades are left alone. The advantage of this procedure is that the perturbations introduced into the flow die out with the time advancing so that the free vibrations are almost unaffected by any perturbation that comes from the flow-field and the vibration curves look much more uniform. The basic idea of this method is illustrated in FIG. 8 which shows exemplarily the resulting normalised displacement of the computation for IBPA=+120° (FTW). From here on all displacement plots are normalised with respect to the maximum displacement.

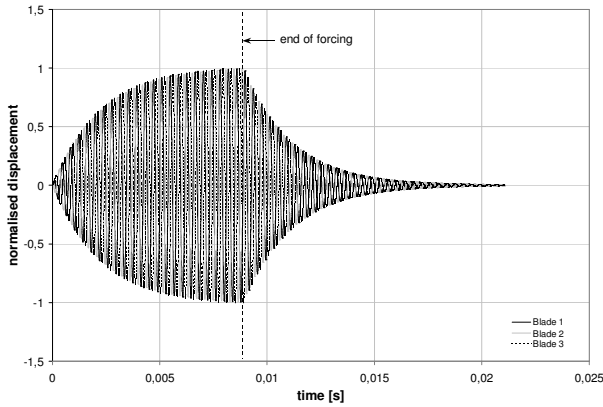


FIG. 8. Displacement for IBPA=+120°

While the damping can be determined with the help of the logarithmic decrement in the interval of the free vibration as describe for method a) the determination is also possible at the end of the forcing period by evaluation of the work done per cycle [22]. Here the blades move with constant amplitude which enables us to construct a force-displacement hysteresis that leads to a relation between the work done by the blade and its maximum stored energy and thus to the loss coefficient for a blade with unseparated flow in the form of

$$(11) \quad \eta \approx \frac{W_d}{2\pi \cdot U_{\max}}$$

with the work done per cycle $W_d = \oint F_L du$ and the maximum kinetic energy $U_{\max} = \frac{1}{2} m \hat{v}^2$. According to

$$\text{equation (10) the damping ratio results from } D = \frac{\Lambda}{2\pi} = \frac{\eta}{2}.$$

On the contrary to the first method we are now able to determine the aerodynamic damping with two different means for the results of one calculation. Within the discussion of the results the different methods are referred to as the *logdec-method* meaning the damping determination by evaluating the logarithmic decrement

and the *integral-method* meaning the determination of the work done per cycle.

A third method for the determination of aerodynamic damping (as well as damping in general) is the so called half-power bandwidth method. It supposes the blade vibration to be dominated by the vibration mode corresponding to the resonance frequency in the vicinity of the resonance frequency. As only one mode is regarded in this work, this assumption is not necessarily needed. The method bases on the frequency response function (FRF) $V_i(\Omega)$ of the i -th mode which can be obtained by FOURIER-Transformation of the time dependent displacement signal as illustrated in FIG. 8.

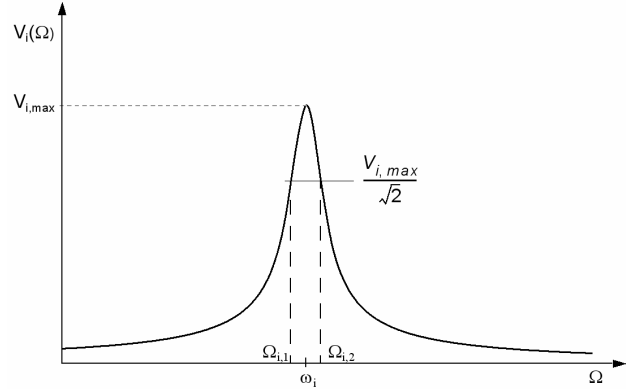


FIG. 9. FRF of single degree of freedom model

First the resonance peak of the FRF plot is detected. The corresponding maximum value of the FRF is $V_{i,max}$. Then the two frequencies $\Omega_{i,1}$ and $\Omega_{i,2}$ are detected where the value of the FRF has decreased to $V_{i,max} / \sqrt{2}$ which leads to the so called bandwidth $\Omega_{i,2} - \Omega_{i,1} = \Delta\Omega$. The damping ratio of the i -th mode can now be derived from the following formula:

$$(12) \quad D_i = \frac{\Omega_{i,2} - \Omega_{i,1}}{\Omega_{i,2} + \Omega_{i,1}}$$

In numerical simulations the discrete displacement signal leads to a discrete frequency response function as well which might result in a more difficult determination of the peak value. In such cases spline functions are very helpful to improve the peak search ability. Additionally the frequency solution is directly depending on the over all calculation time. For economical reasons the calculation times are minimized as far as possible. Moreover is the time of the decaying vibration determined by the amount of the aerodynamic damping which is present and therefore only short time-values can be realised. As a result the frequency resolution gets not better than 35Hz in reasonable calculation times which makes this method unattractive for the determination of aerodynamic damping and this is why it is not used within the current work.

This method is often used for determination of eigenfrequencies as well. Due to the previously described drawbacks (mainly because of the poor frequency resolution) the frequency determination is done by analysing the time periods of succeeding vibration cycles.

2.1.2. Unidirectional Coupling

The second method of the preceding section brings up another idea of how to determine the aerodynamic damping. The unidirectional coupling bases upon some assumptions, they are

- The aerodynamic damping remains constant within the range of small displacements.
- The unsteady lift force depends only on the blade vibration amplitude.

With the fulfilment of those requirements it is possible to define the blade movement independently from the surrounding airflow. This can be achieved in two different ways. The first one still features the MpCCI-coupling interface, which is adapted in a way that only the blade displacements are exchanged while the structural model remains unaffected by the fluid forces.

Using ABAQUS, the blade movement can be realised in two ways. By giving the blades initial conditions as described with equations (6) and (8) the blades perform free vibrations which remain undamped because of the not coupled fluid forces. Another possibility is to use the forcing employed in the first period of method b) with the bi-directional coupling or an equivalent method to create a harmonic blade movement. Both methods result in the same phase shifted blade vibrations while the second method advantages the smaller effort concerning model set-up.

Obviously the use of a FEM solver is not absolutely necessary concerning the simplified model using an unidirectional coupling. The blade movement can be achieved with FLUENT only as well. With the help of so called **User Define Funcions** (UDF) it becomes possible to prescribe a harmonic blade movement. The advantage of this method is the missing displacement-interpolation between the two codes which is basically non-conservative.

Similar to method b) of the bi-directional coupling the unidirectional coupling results in a set of displacement and lift curves which enable us to determine the relation between the work done per cycle and the maximum kinetic energy within one vibration cycle, equation (11).

3. RESULTS

All following results presented in this section have been calculated with a constant timestep size corresponding to a temporal resolution of 110 timesteps per vibration cycle concerning the structural model as well as the flow model. Starting point of the following considerations are the bi-directional coupled calculations using MTO boundary conditions.

As done in the previous section (2.1.1), the next two charts refer to the results of the calculation for $IBPA=+120^\circ$. All charts showing damping ratios are consequently normalised with respect to the overall maximum damping ratio which corresponds to the value determined with the method evaluating the work done per cycle for $IBPA=180^\circ$. The first chart (FIG. 10) illustrates

the averaged, normalised damping ratio versus the number of calculated vibration cycles of the two in chapter 2.1.1 presented methods of damping determination for bi-directional coupled calculations. The dashed, vertical line indicates the end of the forcing and thus the beginning of the decaying vibration (see FIG. 8). During the forcing period the damping is determined using the integral approach. Due to the first cycle(s) the damping ratio decreases from a comparatively high value down to an expected steady value. Considering equation (1) it becomes obvious that all blades with $k \neq 0$ start with an initial non-zero displacement. These displacements lead to perturbations which are responsible for this inherent error. In the period of the decaying vibrations the method becomes unstable which is indicated by an increase in the damping ratio at the end of the forcing period. The method employing the logarithmic decrement provides better results for this period but it fails during the forcing period. The increasing vibration amplitudes lead to negative logarithmic decrements which theoretically becomes zero when a constant vibration amplitude is reached. The main conclusion is, that both methods supply equivalent results for $IBPA=+120^\circ$ which doesn't imply a general regularity yet.

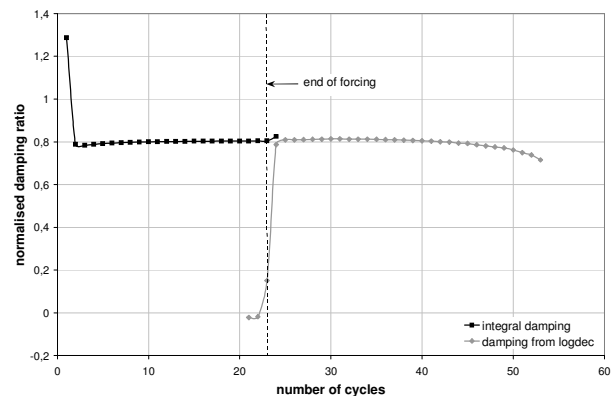


FIG. 10. Normalised damping ratio versus number of cycles

For the same case set up FIG. 11 shows the averaged, normalised frequency versus the calculation time. All frequency values are normalised using the eigenfrequency of the undamped system which is indicated by the horizontal line. As expected the frequency of the aeroelastic system converges to the desired, forced structural eigenfrequency. After the forcing has finished the aeroelastic system responds in its own frequency.

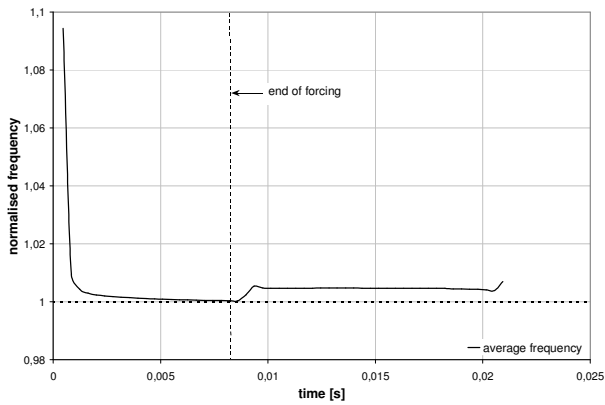


FIG. 11. Normalised frequency versus time

The following figure shows exemplarily for $IBPA=+120^\circ$ the averaged displacement envelopes (only the maximal displacements are included) versus number of cycles of the two different methods of blade movement described in chapter 2.1.1. While the forced blade vibration takes approximately 23 cycles before the desired amplitude is reached (main disadvantage), the initial blade movement immediately starts with the desired amplitude. For reasons of comparison the moments where the decaying vibrations start are brought into correlation. Especially in the beginning both envelopes correlate quite well, while the initial perturbations caused by methodical problems of the initial blade movement generation lead to increasing differences in the displacements.

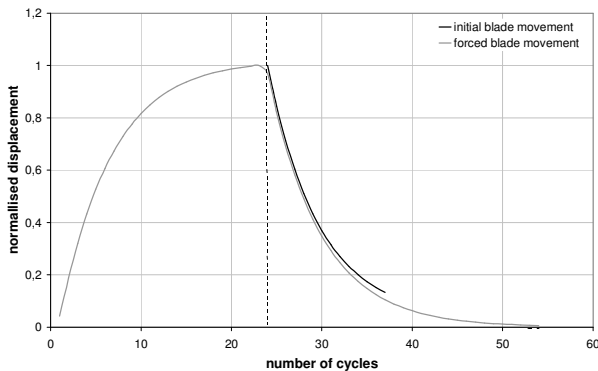


FIG. 12. Normalised Envelopes of different blade movement methods ($IBPA=+120^\circ$)

After the consideration of a single interblade phase angle has been discussed the results of major interest are going to be presented. These contain the results of coupled calculations of eight different $IBPA$'s ($0^\circ, \pm 72^\circ, \pm 90^\circ, \pm 120^\circ$ and 180°) of up to five-passage calculations. FIG. 13 and FIG. 14 display the normalised aerodynamic damping ratio (identified with four different methods) versus the interblade phase angle. Firstly FIG. 13 shows the results obtained with those methods when using standard boundary conditions (referred to as reflecting boundary conditions – RBC). The trend observed with the closer consideration of $IBPA=+120^\circ$ is supported by comparison of the results of the forced, bi-directional calculations where the damping has been determined by making use of the integral method and the logdec-method. Both yield identical results and can be regarded as equivalent. Additionally the results of the unidirectional coupling are given (damping determination

only with the integral method). The results correlate very well with the results of the bi-directional coupling which is due to the relatively small displacement. Considering the bi-directional forced vibration calculations an equilibrium between forcing and fluid forces develops until the end of the forcing period. Within this state of equilibrium the blade vibrates with a constant amplitude which can be easily imitated by making use of a unidirectional coupling with the same vibration frequency. Therefore similar results appear to be feasible. Considering the initial blade movement at first only the $IBPA=+120^\circ$ has been analysed whose result correlates very well with the rest of the calculations (see also FIG. 12). FIG. 13 also reveals the known asymmetry of damping graphs for the 1st flap mode where the global minimum is typically associated with low positive interblade phase angles.

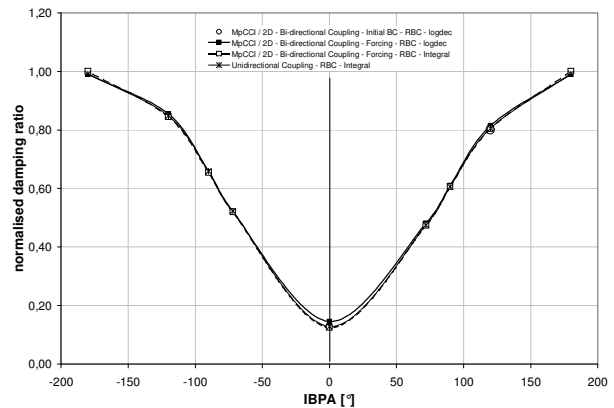


FIG. 13. Normalised damping graphs, RBC

The effect becomes even more clearly when switching to non-reflecting boundary conditions (NRBC). The damping of the positive interblade phase angles decreases even more while the damping of the negative interblade phase angles increases which both contributes to the asymmetry of the curve. The global minimum can not be reliably determined because of a lack of small interblade phase angle calculations. The conclusions made for the different calculations methods remain valid.

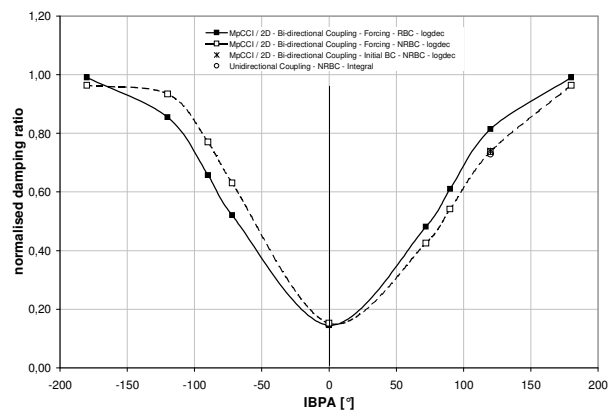


FIG. 14. Normalised damping graphs, RBC vs. NRBC

The following diagram shows the normalised frequencies of the aeroelastic system obtained from the bi-directional calculations versus interblade phase angle. The curves of RBC- and NRBC-calculations show similar results. The visible differences seem to increase with the $IBPA$ increasing too. What catches the eye is that the

frequencies are increasing as well. The influence of stiffening effects is possibly less intensive than the effect of moving air masses with small interblade phase angles. With greater interblade phase angles this behaviour seems to work vice versa. Independent from the type of boundary condition used, the results obtained with initial blade movement obviously differ quite a lot from the rest of the results which is most likely due to those perturbations caused by the initial blade movement.

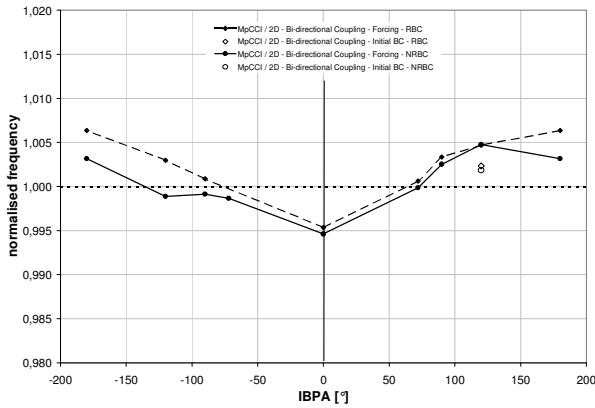


FIG. 15. Normalised frequencies, MTO, RBC vs. NRBC

Finally FIG. 16 and FIG. 17 contain the results of bi-directional, forced calculations with RBC for cruise conditions¹ in comparison to the MTO-results. The damping curve belonging to the cruise condition is below the one corresponding to the MTO condition which is quite obvious because of the lower pressure level associated with the cruise condition.

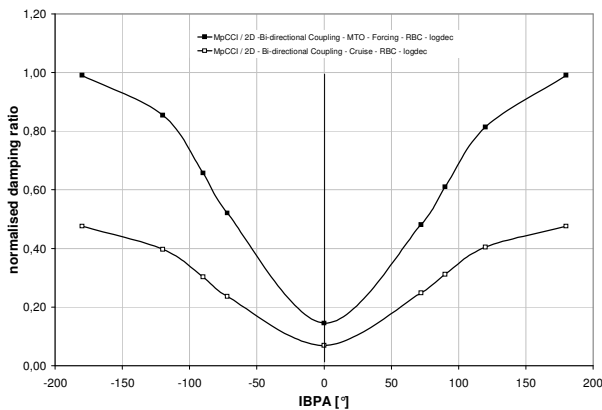


FIG. 16. Normalised damping graphs, RBC, MTO vs. Cruise

According to the reduced damping level the change in frequency also decreases as expected.

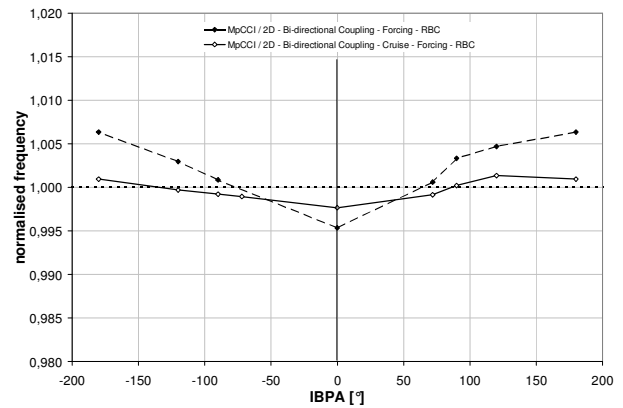


FIG. 17. Normalised frequencies, RBC, MTO vs. Cruise

4. CONCLUDING REMARKS

The Fluid-Structure-Coupled simulations have been carried out using different methods for the blade movement as well as for the determination of the aerodynamic damping. Although different physical and numerical assumptions have been applied, good correlation could be demonstrated for the different methods used herein. In the first instance it can be noticed that bi-directional and unidirectional results correlate very well within a range of small displacement amplitudes. Different methods of blade movement have been used and have been shown to be equivalent concerning damping determination going along with an immense potential of saving computational time with initial blade movement. The only difference was observed with the results of vibration frequency for the initial blade movement whereas the completion of the calculations of initial blade movement should be carried out for the rest of the investigated interblade phase angles. Moreover could be demonstrated that the results essentially depend on the choice of the type of boundary conditions as with NRBCs turned on the damping curve develops its characteristic shape with the positive interblade phase angles being damped more than their negative counterparts. Talking about frequency determination it can be found that different types of boundary conditions may affect the results depending on the value of the interblade phase angle.

Although similar damping results were gained using unidirectional and bi-directional coupling calculations, the bi-directional coupling is of greater interest for the identification of aerodynamic elements for the EBM. With the help of known values like forcing, aerodynamic damping and the corresponding displacement amplitude it is possible to identify parameters for the aerodynamic elements. The difference between structural vibration frequency and aeroelastic vibration frequency leads to a possibility of how to identify a moving air mass [5].

¹ The temporal resolution was changed to 220 timesteps per vibration cycle.

5. REFERENCES

- [1] ABAQUS User's Manual to Version 6.51
- [2] Beirow B., Kühhorn A., Schrape S., Blisk Vibration Phenomena in Consideration of Fluid Structure Interaction. Proc. of 11th Int. NAFEMS World Congress, Vancouver 2007
- [3] Beirow B., Kühhorn A., Golze M., Klauke Th., Strukturdynamische Untersuchungen an Hochdruckverdichterschaufelscheiben unter Berücksichtigung von Mistuningeffekten, VDI-Schwingungstagung 2004, Modalanalyse und Identifikation, VDI-Berichte Nr. 1825, 2004
- [4] Beirow B., Kühhorn A., Golze M., Klauke Th., Parchem R., Experimental and Numerical Investigations of High Pressure Compressor Blades Vibration Behaviour Considering Mistuning. NAFEMS World Congress, St Julians, Malta, 2005
- [5] Beirow B., Kühhorn A., Schrape S., Influence of Airflow on Blisk Vibration Behaviour, 1. CEAS European Air and Space Conference, Berlin, 2007
- [6] Cumpsty N.A., Compressor Aerodynamics, Reprint Edition, Krieger Publishing Company, Malabar 2004
- [7] Ewins D.J., Modal Testing, Second Edition, Research Studies Press Ltd., 2000
- [8] Fluent 6.2 - User's Guide, Fluent Inc. 2005
- [9] Gasch R., Knothe K., Strukturdynamik - Band 1 - Diskrete Systeme, Springer Verlag Berlin, 1987
- [10] Gasch R., Knothe K., Strukturdynamik - Band 2 - Kontinua und ihre Diskretisierung, Springer Verlag Berlin, 1989
- [11] Giles M., A Numerical Method For The Calculation Of Unsteady Flow In Turbomachinery, GTL Report Nr. 105, 1991
- [12] Glück M., Ein Beitrag zur numerischen Simulation von Fluid-Struktur-Interaktionen- Grundlagenuntersuchungen und Anwendung auf Membrantragwerke, Dissertation, Shaker Verlag Aachen, Erlangen 2003
- [13] He L., Method of Simulating Unsteady Turbomachinery Flows with Multiple Perturbations, AIAA Journal, Vol. 30, No. 11, 1992
- [14] Hurka J., Numerische Untersuchung zur Aeroelastik dünner Platten, Dissertation, RWTH Aachen, 2002
- [15] Imregun M., Sayma A. I., Sbardella L., Semi-structured Meshes for Axial Turbomachine Blades, International Methods for Numerical Methods in Fluids, 32(5), S.569-584, 2000
- [16] Imregun M., Sayma A. I., Vahdati M., Multi-Stage Whole Annulus Forced Response Predictions Using An Integrated Non-Linear Analysis Technique - Part I: Numerical Model, Journal of Fluids & Structures, 14(1), S. 87-101, 2000
- [17] Imregun M., Sayma A. I., Vahdati M., Multi-Stage Whole Annulus Forced Response Predictions Using An Integrated Non-Linear Analysis Technique - Part II: Study of A HP-Turbine, Journal of Fluids & Structures, 14(1), S. 103-125, 2000
- [18] MpCCI Technical Reference Version 3.0, Fraunhofer Institut, 2004
- [19] Poinot T.J., Lele S.K., Boundary Conditions for Direct Simulations of Compressible Viscous Flows, Journal of Computational Physics 101, S. 104-129, 1992
- [20] Schrape S., Kühhorn A., Golze M., Simulation of Fluid Damped Structural Vibrations using a Partitioned Coupling Approach via MpCCI, Tagungsband des 3. NAFEMS CFD-Seminar: Simulation gekoppelter Strömungsvorgänge (Multifield FSI), Wiesbaden, 08. - 09. Mai 2006
- [21] Steindorf J., Partitionierte Verfahren für Probleme der Fluid-Struktur Wechselwirkung, Dissertation, TU Braunschweig, 2002
- [22] Thomson W.T., Theory of Vibration with Applications, Prentice Hall, 1972